

Seismic Fragility Analysis of Base-Isolated Buildings resting on Sloping Ground under real earthquake ground motions

Abhishikta Chanda¹, and Rama Debbarma²

Abstract:


Most of the hilly regions are situated in high seismic zones of India. Such a threat compels the need to keep a check on the performance of buildings that suffer extensive damages or even collapse during strong ground shaking on account of near-fault pulses. The present research work is related to the construction of an ensemble of fragility curves for buildings lying on 15°, 30° and 45° slopes. In order to mitigate the damages caused by near-field earthquakes, base isolation system using lead rubber bearing has been provided at the foundation level. The responses of the buildings are obtained by incremental dynamic analysis and linear regression is performed to obtain the probabilistic seismic demand models to find out the median intensity and the uncertain parameters. All the buildings have been analyzed for slight, moderate, extensive and collapse damage states for which the corresponding fragility curves are obtained. Base isolator was able to significantly reduce the seismic demand measures by imparting flexibility to the system and therefore can be recommended as an alternative to conventional fixed base type buildings located on sloping terrain experiencing near-fault motions.

Keywords: Base isolation system, near-field earthquakes, incremental dynamic analysis, demand measures, sloping ground.

1.1 Introduction

The geographical topography of an area often determines the configuration of a structure. In most of the cases, it is not feasible to construct regular buildings in sloping terrain. In order to satisfy the increasing demand of commercial and residential growth, rapid urbanization is being made in hilly regions despite of the irregularities induced in R.C framed buildings. The angle of inclination of the slope will result in the difference in the height of columns that will impart both mass and stiffness irregularity. Shorter columns attract larger lateral forces proportional to its bending stiffness than longer ones and because of this there is concentration of shear force in the relatively short columns which fail before the long columns (Duggal, 2013). Most of the hilly regions are within severe to very severe seismicity zones of India for which, buildings on sloping ground are quite vulnerable to earthquake shaking. Regions located near to active faults experience near-field (NF) earthquakes that possess high energy pulses accompanied with higher amplitudes of acceleration and velocity, permanent ground displacement and short duration impulses by Heydari and Mousavi (2015). The catastrophic impacts of NF motions on hill buildings will be beyond our comprehension if appropriate estimation of the seismic responses is not

adequately made prior to any earthquake event. A parametric study between 5 storey and 10 storey buildings on plain ground with the performance of similar buildings located on slopes of 23° and 27° under the effects of Chamoli earthquake and Uttarkashi earthquake was performed to compare the effects of near and far field earthquakes (Shah, 2014). The outcome of the experiment was that base shear induced in 10 storey due to Chamoli near-field was 200% more in 23° slope and 47% more in 27° slope compared to plain building. Response spectrum analysis of buildings with storey height varying from 4 to 11 with configurations Step back, Set back-Step back and Set back showed that building with Step back configuration was found to be most vulnerable, the short column in the ground storey was the worst affected in case of Set back-Step back, base shear was more on long column and Set back buildings were marked best for construction on sloping ground by Birajdar and Nalawade (2004). In order to overcome the shortcomings in ductile design philosophy, base isolation technology emerged worldwide some 100 years ago to take control over death toll, structural as well as non-structural damages under the impacts of design-basis as well as maximum credible earthquakes. Base isolation is based on the approach of reducing the seismic demand rather than increasing the structural capacity by imparting flexibility to a

 Corresponding author: ramadebbarma@gmail.com.

1. 2Department of Civil Engineering, National Institute of Technology Agartala, India. Tripura-799046, India

2. Dr. Rama Debbarma, Associate professor, Department of Civil Engineering, National Institute of Technology Agartala, Tripura – 799046, India

building. It is done by inserting structural elements like elastomeric rubber bearings with low horizontal stiffness arranged in layers interposed between steel shims that possess very high vertical stiffness at the foundation level. By doing so, both the isolator and the superstructure gets deflected by the dynamics of the system resulting in the increase in fundamental time period of the building more than the predominant frequency of the ground motions, thereby evading disastrous effects of resonance (Chopra, 1981; Naeim and Kelly, 1999). The vertical stiffness enables the base isolators to carry heavy weight of the superstructure, control bouncing effect of vertical ground motions and also helps to confine the rubber from bulging out. The lowering of the fundamental frequency by the isolation system, in turn lengthens the time period, reduces storey-drift in the superstructure and some amount of reduction in acceleration (FEMA 356:2000). The experiment has been conducted with four types of base isolators namely Linear rubber bearings (LinRB), High-Damping rubber bearings (HDR), Lead rubber bearing (LRB) and Electricite-de-france (EDF) to check the most suitable isolator to be used for near-fault ground motions. A comparative study has been performed between base isolated and fixed base building frames on 25°, 30° and 35° sloping ground using lead rubber bearing as the isolation system (Sumana et al., 2016). Maximum storey drift was obtained on 25° and minimum on 35° which were within the storey drift limit i.e. 0.004*h, h being the storey height unlike fixed base. Base shear averagely decreased by 55% with the increase in slope for the base isolated building. Jangid and Kelly (2001) found out that near-fault motions consist of significant energy at high frequency in addition to pulse-type displacements and EDF type was the optimum choice for near-fault sites. However, lead rubber bearing (LRB) is particularly used as base isolators for practical purposes on account of its low cost, vertical support, horizontal flexibility and damping by plastic deformation of lead which enhances the performance of buildings (Robinson, 1982). The performance of base-isolation system of a 4-storey building using bi-directional time histories of Kobe, El Centro and Northridge earthquakes which resulted in reduction of peak base shear, peak top floor acceleration and roof-drift ratio has been investigated (Gomase and Bakre, 2011; Salic et al., 2008; Darji and Purohit, 2006; Keerthana et al., 2014). Earthquake forces are complex, irregular comprising of sinusoidal waves of several frequencies with varying amplitudes. The random nature is associated with various uncertainties depending upon several factors like its characteristics that include intensity, duration, frequency etc., nature of rupture of fault plane, seismic transmission path and soil conditions. Each of these uncertain parameters has significant impact on the seismic

performance of a structure (FEMA P-58). Similarly, uncertainties exhibited by structures in the form of mechanical properties of materials, some degree of modeling idealization, have resulted in probabilistic seismic assessment of structures which provides a realistic estimation of structural vulnerability during earthquakes (Shinozuka et al., 2000; Hwang and Low, 1989). Fragility analysis is a probabilistic approach to the risk assessment of structures using fragility curves as one of its outcomes to describe a structure's vulnerability or satisfactory performance under some predefined threshold limits when subjected to earthquakes, hurricanes or any other extreme loading condition (Ghosh et al., 2017). The first methodology has been proposed for performing seismic fragility analysis for nuclear power plants (Reed and Kennedy, 1994). The fragility equation $F_R(x)$ was modelled as two-parameter lognormal distribution function by Ellingwood and Kinali (2009), expressed as: $F_R(x) = P[LS|Q = x] = \phi\left[\frac{\ln x - \ln m_R}{\beta_R}\right]$ where, $\phi[\]$ is the standard normal probability integral; LS is the limit state capacity; Q is the intensity of seismic demand, x is any ground motion intensity and m_R and β_R are the median capacity and lognormal standard deviation respectively. Generally for moderate shaking, seismic demand parameters are often correlated to Peak Ground Acceleration (PGA) as the ground motion intensity by Rani and Singh (2018). Obtaining the seismic vulnerable parameters is the first step to construct fragility curves which is done by capacity spectrum method or by non-linear dynamic analysis. They have performed Incremental dynamic analysis (IDA) under an ensemble of multiple scaled accelerogram records of earthquake ground motions with a minimum of 3 to 7 records, to predict the intensity level at which each chosen earthquake produces a complete range of structural behavior starting from elasticity to yielding and finally collapse by Vamvatsikos and Cornell (2002). The scarce availability of literature review on base-isolated buildings located on hilly regions forms a basis of the present research work to tackle the disastrous effects of strong near-field ground motions.

1.2 Methodology In the present study, the models are analysed by Incremental Dynamic Analysis to generate the performance parameters and the probabilistic demand models are obtained by least square regression technique. The methodology is explicitly described below:

Time histories of seven NF real earthquake records have been used to perform IDA for both FB and BI buildings with Peak Ground Acceleration (PGA) as the intensity measure (IM) scaled uniformly from 0.1g to 1g at an increment of 0.1g. The performance parameters which get affected during an event of earthquake are the demand measures (DM). The DMs considered for the parametric study are: (a) Maximum

inter-storey drift ratio (MISDR) (b) Maximum base shear (MBS) and (c) Maximum top floor acceleration (MTFA). The responses of IDA are plotted between lognormal DMs in X-axis.

Linear regression helps to establish a probabilistic relationship between the performance parameters and IM (Shome and Cornell, 1999). They have formulated a direct correlation between DM and IM which forms the basis of construction of fragility curves (Baker and Cornell, 2006). The relationship is given as:

$$DM = x X^y \tag{1}$$

Taking lognormal on both sides of equation (1)

$$\ln(DM) = \ln(x) + y \ln X \tag{2}$$

Where x and y are the regression coefficients.

From the probabilistic seismic demand models (PSDMs), the threshold intensities are found out to evaluate the probability by which the vulnerable parameters i.e. DM, exceeds the threshold value for any given intensity of earthquake shaking by undergoing slight, moderate, extensive or collapse damages.

The performance of base-isolated buildings under slight, moderate, extensive and collapse damage states whose threshold limits are indicated in Table 1 for corresponding damage measures (Bhandari et al., 2019).

Table 1 Threshold values for different damage states and damage measures

Damage Measures	Damage States			
	Slight	Moderate	Extensive	Collapse
MISDR	0.0005	0.001	0.002	0.007
MBS	0.05W	0.1W	0.15W	0.2W
MTFA	0.1g	0.2g	0.3g	0.4g

In the present study, the Probability of exceedance is expressed as a lognormal cumulative probability distribution function as:

$$P_f(D \geq C/IM = X) = \Phi\left(\frac{\ln\left(\frac{x}{\mu}\right)}{\Delta_T}\right) \tag{3}$$

Where P_f represents the probability that the ground motion with $IM=X$ will initiate slight, moderate, extensive or collapse damages in the structure, $\Phi(\cdot)$ represents the standard cumulative normal distribution function obtained from cumulative normal distribution table, μ is the median value of X and Δ_T is the total standard deviation expressed as:

$$\Delta_T^2 = \Delta_D^2 + \Delta_C^2 \tag{4}$$

Δ_D is the uncertainty in seismic input motion i.e. record-record variability and Δ_C is the uncertainty in structural capacity which is taken as 0.3 for both BI and FB.

1.3 Numerical Example

The present study was investigated with six step-back models, three of which has fixed base configuration while the other three has isolated base, situated on slopes of 15°, 30° and 45°. Description of the buildings, base-isolator used and details of the ground motions have been mentioned in further sub-sections.

1.3.1 Structural Modelling

The buildings are G+5 of 18m height having 4 bays on both X and Y-direction in plan spaced at 3m each. Beams are 0.4mX0.5m and columns are

0.5mX0.5m cross-section. The rigid beam located at the isolation level is 0.5mX1m. Slabs are 0.125m in thickness. The structural elements are made up of M30 grade of concrete and Fe500 grade of steel. The gravity loads considered are dead loads of each structural element and live load of 3.5 kN/m² on floors. Wall loads have been assigned as uniformly distributed loads on beams with unit weight of brick as 20 kN/m³. The thickness of the exterior walls is assumed to be 0.250m and interior walls as 0.125m with 1m height of parapet. The hill buildings are assumed to be special moment resisting frames located in seismic zone V with medium soil type, all of which are in accordance to (IS1893(Part-I)-2016). The real earthquake data has been selected as per IS 1893(Part-I) -2016 for zone v, which is having effective peak ground acceleration of 0.36g for the maximum considered earthquake(MCE) and 0.18g for design basis earthquake (DBE). Modelling and analysis was performed inSAP2000 software. The models are abbreviated as:

- i. FB-15°: Fixed Base building inclined at 15°
- ii. BI-15°: Base-Isolated building inclined at 15°
- iii. FB-30°: Fixed Base building inclined at 30°
- iv. BI-30°: Base-Isolated building inclined at 30°
- v. FB-45°: Fixed Base building inclined at 45°
- vi. BI-45°: Base-Isolated building inclined at 45°

The Plan of Fixed base and Base-Isolated building is shown in Fig.1. The elevations of models are shown in Fig.2. The highlighted portions in Figs. 1 and 2 have been chosen for analysis and calculations.

ORIGINAL RESEARCH

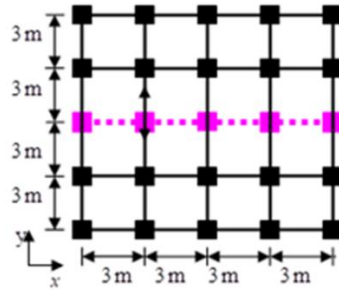


Fig. 1 Plan of Fixed base and Base-Isolated buildings

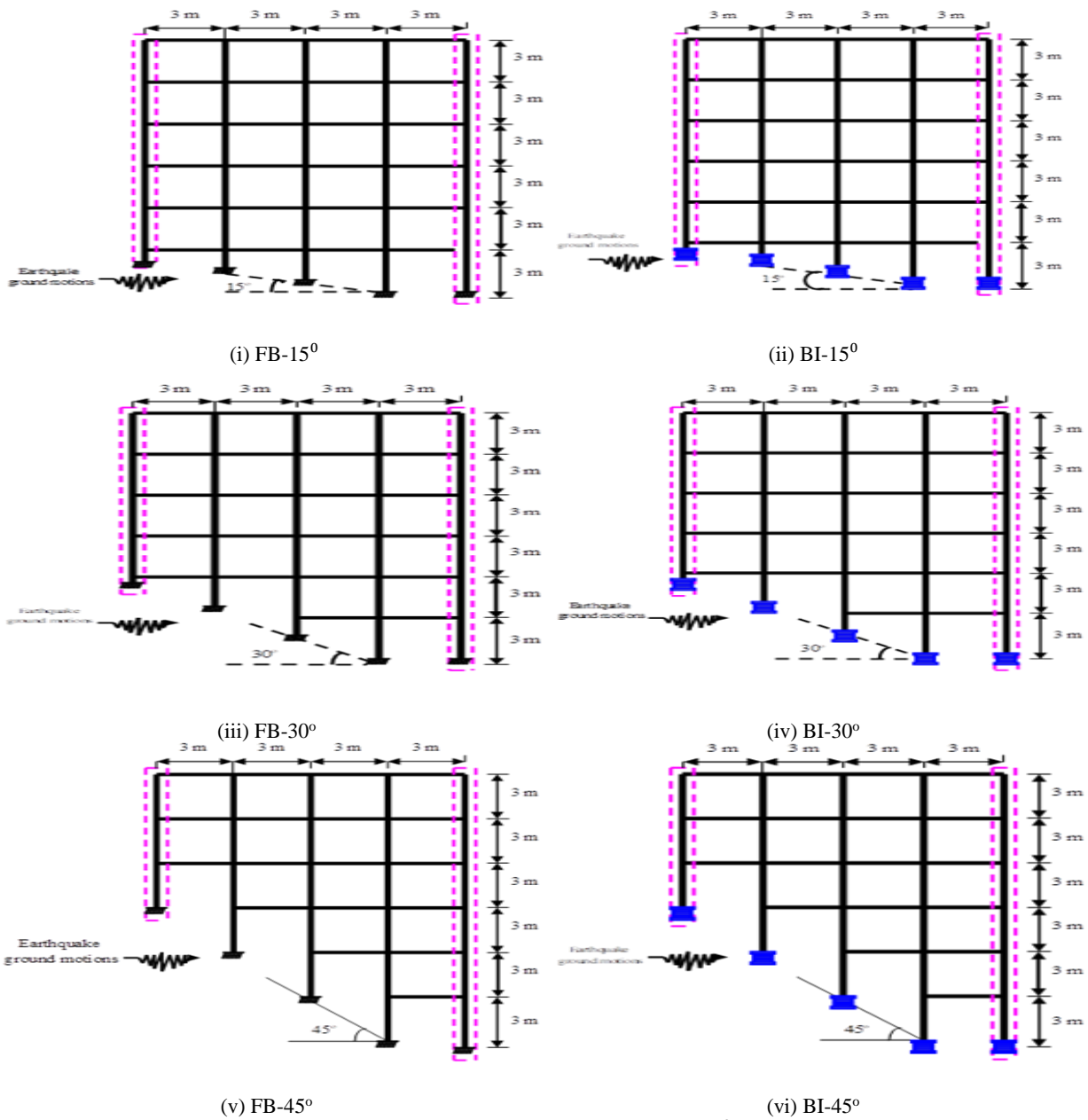


Fig. 2 Elevation of Fixed base and Base-Isolated buildings resting on 15°,30° and 45° hill slopes.

1.3.2 Modelling of the base-isolation system

The modelling of Lead rubber bearing (LRB) has been done in SAP2000 and the isolator design parameters were referred from the guidelines laid down by UBC-1997. The step by step design to determine the optimum configuration of the isolator was proceeded from (Naeim and Kelly, 1999). Seismic coefficient $C_{VD}=0.54$ and Damping coefficient $B_D=1.2$ for effective damping $\beta_d=10\%$ have been obtained as per code. The elementary properties given as inputs are as follows:

The design displacement of the isolator is given by:

$$D_D \square \frac{g}{4\gamma^2} C_{VD} \frac{T_D}{B_D} \tag{5}$$

where seismic coefficient $C_{VD}=0.54$, damping coefficient $B_D=1.2$ for effective damping $\beta_d=10\%$ and T_D being the design fundamental time period of the isolator assumed as 2.5secs.

The effective stiffness, horizontal stiffness and the vertical stiffness of the isolator are expressed as:

$$K_{eff} \square \frac{W \square 2\gamma \square^2}{g \square T_D \square}, K_H \square \frac{G A_{LRB}}{t_r} \text{ and}$$

$$K_r \square \frac{E_c}{t_r} A_{LRB} \tag{6}$$

where W is the maximum support reaction at the base of column;
 g is the acceleration due to gravity; T_D is assumed to be 2.5secs which is the fundamental time period of the isolator, G is the shear modulus of rigidity; E_c is the instantaneous modulus of compression of rubber-steel

composites, A_{LRB} is the area of bearing and t_r is the total thickness of rubber.

The yield displacement and yield strength of rubber are computed from equation (7) respectively

$$D_y = \frac{Q}{K_1 - K_2} \text{ and } F_y = Q + K_2 D_y \tag{7}$$

where Q is the characteristic strength; K_2 and K_1 are the post and pre stiffness respectively; K_1 being 10 times of K_2 and their ratio is termed as post yield stiffness ratio. D_D and D_y are 0.279m and 0.0057m respectively.

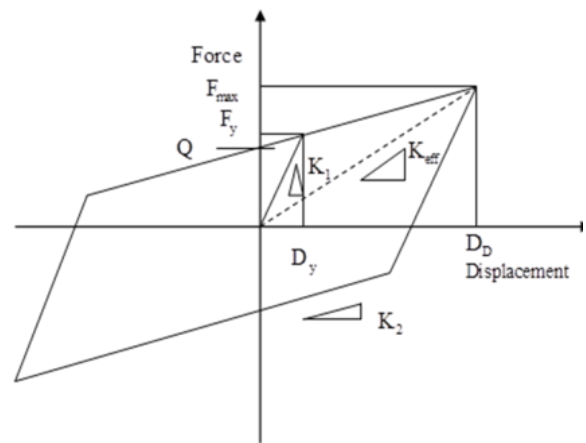


Fig. 3 Bilinear Force-Displacement relationship of LRB used in BI-15°, BI-30° and BI-45° buildings

Table 2 Bilinear characteristics of lead rubber bearing

Model Type	Isolator Properties								
	W (kN)	U ₁ (kN/m) (K _V)	U ₂ (kN/m)		U ₃ (kN/m)		F _y (kN)	Q (kN)	A _h (m ²)
			Linear (K _{eff})	Non-linear (K _I)	Linear (K _{eff})	Non-linear (K _I)			
BI-15°	1060	231126.6	682.52	5753.11	682.52	5753.11	33.29	29.97	32.82
BI-30°	1000	218044	643.88	5427.46	643.88	5427.46	31.40	28.27	30.96
BI-45°	1000	218044	643.88	5427.46	643.88	5427.46	31.40	28.27	30.96

where U_1 , U_2 and U_3 represent the stiffness along z, x and y directions respectively and A_h is the area of the hysteresis loop. The properties of LRB used for the modelling of the isolator are given in Table 2.

1.3.3 Attributes of Near-field motions

Table 3 Characteristics of NF Earthquakes:

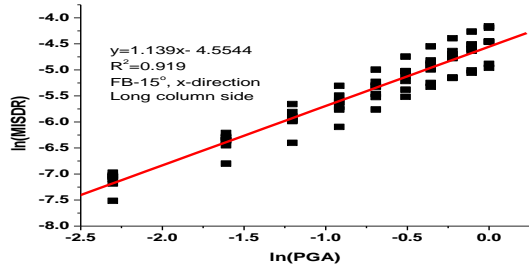
SI no.	Year	Name of earthquake	Station name	Magnitude	PGA (g)	Distance (km)
				Mw		
1.	1979	Imperial Valley	El Centro #4	6.5	0.349	8.3
2.	1994	Northridge	White Oak Church	6.7	0.444	12.9
3.	1995	Kobe	KJMA	6.9	0.821	1
4.	1984	Morgan Hill	Gilroy Array #6	6.2	0.280	6.1
5.	1971	San Fernando	Los Angeles	6.6	0.249	16.5
6.	1992	Landers	Joshua Tree	7.4	0.278	10.3
7.	1989	Loma Prieta	Saratoga	7	0.316	4.1

The earthquake load applied to the buildings includes time histories of seven NF motions. The NF earthquakes selected have magnitudes greater than 6 on Richter scale located within 17 km of nearest fault. The database was extracted from Center for Engineering Strong Motion Data.

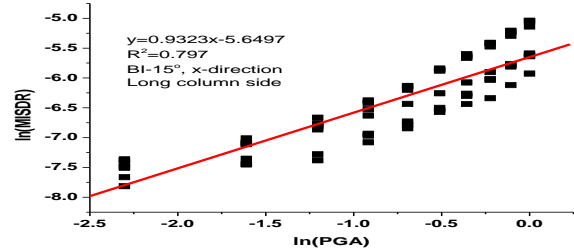
1.4 Results and discussion

Linear regression is performed on the plot of log-normal DMs in terms of Maximum inter story drift ratio (MISDR), maximum base shear (MBS) and maximum top floor acceleration (MTFA) against log-normal PGA to obtain a relationship between the two parameters which would generate the PSDMs. The Plots of MISDR, MBS and MTFA of (a) Fixed base and (b) Base-Isolated building along X-direction inclined at 15° slope angle considering NF ground motions as shown in Fig.4. Similar Linear regression has been performed for fixed base and base isolated building inclined at 30° and 45° slope angle

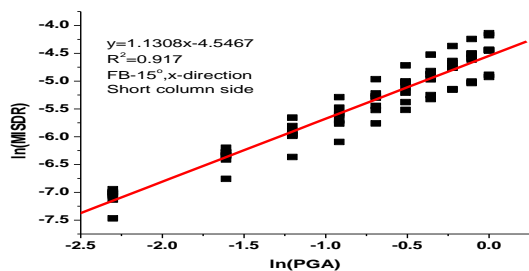
considering NF ground motions. The threshold values of DMs given in Table 1 are used in the PSDMs to obtain the median intensity for the respective DM. The probability of exceedance is obtained from the cumulative normal distribution table when any given intensity exceeds the threshold limit. The PSDMs of various Demand Measures for different models on sloping ground are given in Table 4 and Median values of Intensity Measure (X) for different Damage States for buildings on sloping ground are given in Table 5.



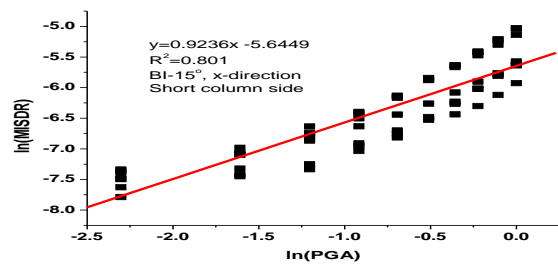
(i) Maximum inter-storey drift ratio along long column



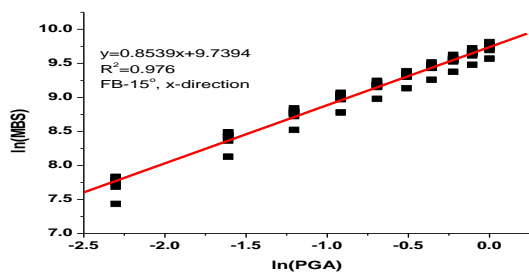
(i) Maximum inter-storey drift ratio along long column



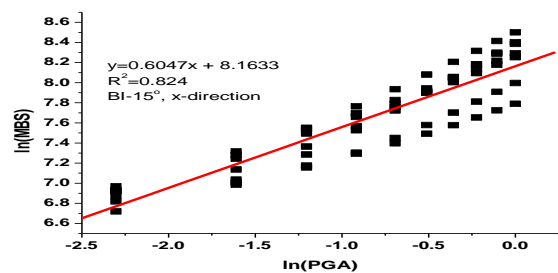
(ii) Maximum inter-storey drift ratio along short column



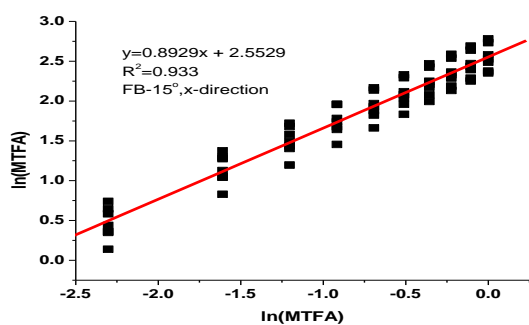
(ii) Maximum inter-storey drift ratio along short column



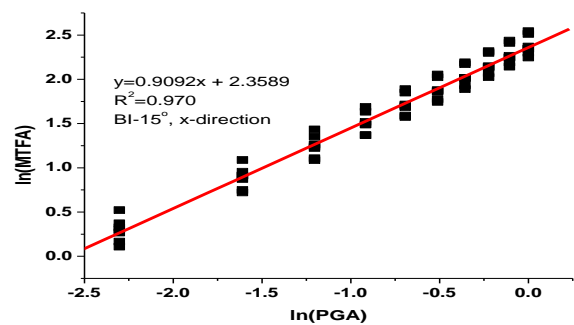
(iii) Maximum base shear



(iii) Maximum base shear



(iv) Maximum top floor acceleration



(iv) Maximum top floor acceleration

(a) Fig. 4 Plot of MISDR, MBS and MTFA of (a) Fixed base and (b) Base-Isolated building along X-direction inclined at 15° slope angle considering NF ground motions.

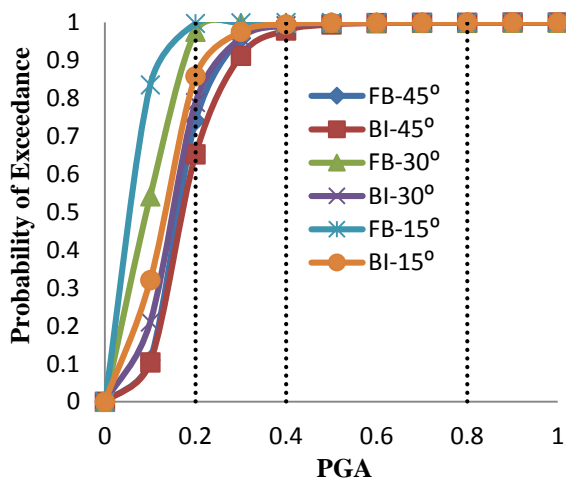
Table 4 PSDMs of various Demand Measures for different models on sloping ground

Direction	Model Type	DM	Response	PSDM	Δ_D	R ²	
X	FB-15 ⁰	MISDR	Long	ln(MISDR)	1.1392ln(PGA)+ln0.010521	0.24	0.919
			Short	ln(MISDR)	1.1308ln(PGA)+ln0.010602	0.24	0.917
		MBS		ln(MBS)	0.8539ln(PGA)+ln16973.35	0.09	0.976
		MTFA		ln(MTFA)	0.8929ln(PGA)+ln12.84429	0.17	0.933
X	BI-15 ⁰	MISDR	Long	ln(MISDR)	0.9323ln(PGA)+ln0.003518	0.33	0.797
			Short	ln(MISDR)	0.9236ln(PGA)+ln0.003535	0.32	0.801
		MBS		ln(MBS)	0.6047ln(PGA)+ln3509.749	0.19	0.824
		MTFA		ln(MTFA)	0.9092ln(PGA)+ln10.57931	0.11	0.970
X	FB-30 ⁰	MISDR	Long	ln(MISDR)	1.1856ln(PGA)+ln0.008032	0.22	0.935
			Short	ln(MISDR)	1.1838ln(PGA)+ln0.008561	0.24	0.926
		MBS		ln(MBS)	0.9154ln(PGA)+ln16645.58	0.07	0.986
		MTFA		ln(MTFA)	0.9243ln(PGA)+ln11.88646	0.18	0.926
X	BI-30 ⁰	MISDR	Long	ln(MISDR)	0.8307ln(PGA)+ln0.002538	0.31	0.776
			Short	ln(MISDR)	0.8406ln(PGA)+ln0.002734	0.32	0.775
		MBS		ln(MBS)	0.6082ln(PGA)+ln3328.576	0.19	0.834
		MTFA		ln(MTFA)	0.9131ln(PGA)+ln10.11784	0.14	0.955
X	FB-45 ⁰	MISDR	Long	ln(MISDR)	1.1434ln(PGA)+ln0.004138	0.22	0.928
			Short	ln(MISDR)	1.2208ln(PGA)+ln0.014485	0.24	0.930
		MBS		ln(MBS)	0.9147ln(PGA)+ln13693.82	0.07	0.986
		MTFA		ln(MTFA)	0.9167ln(PGA)+ln11.10172	0.19	0.916
X	BI-45 ⁰	MISDR	Long	ln(MISDR)	0.7692ln(PGA)+ln0.001956	0.29	0.769
			Short	ln(MISDR)	0.9531ln(PGA)+ln0.005668	0.37	0.762
		MBS		ln(MBS)	0.5620ln(PGA)+ln3276.071	0.17	0.849
		MTFA		ln(MTFA)	0.9035ln(PGA)+ln10.10570	0.16	0.938

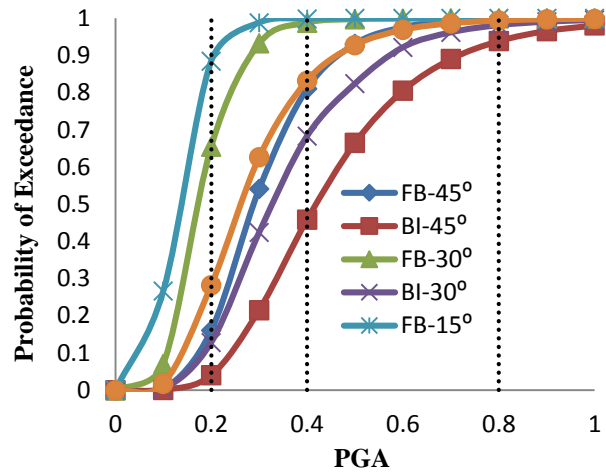
Table 5 Median values of Intensity Measure (X) for different Damage States for buildings on sloping ground

				Damage States				
Direction	Model type	DM		Δr	Slight	Moderate	Extensive	Collapse
					μ	μ	μ	μ
X	FB-15°	MISDR	Long	0.38	0.069	0.127	0.233	0.699
			Short	0.38	0.067	0.124	0.229	0.693
		MBS		0.31	0.036	0.082	0.132	0.184
		MTFA		0.34	0.056	0.122	0.192	0.265
X	BI-15°	MISDR	Long	0.45	0.123	0.259	0.545	2.091
			Short	0.44	0.120	0.254	0.539	2.095
		MBS		0.36	0.161	0.507	0.991	1.595
		MTFA		0.32	0.073	0.157	0.245	0.336
X	FB-30°	MISDR	Long	0.37	0.096	0.172	0.309	0.890
			Short	0.38	0.091	0.163	0.293	0.843
		MBS		0.31	0.042	0.089	0.140	0.192
		MTFA		0.35	0.067	0.142	0.221	0.301
X	BI-30°	MISDR	Long	0.43	0.141	0.326	0.750	3.390
			Short	0.44	0.132	0.302	0.689	3.059
		MBS		0.35	0.162	0.506	0.985	1.581
		MTFA		0.33	0.077	0.166	0.259	0.354
X	FB-45°	MISDR	Long	0.37	0.157	0.289	0.529	1.583
			Short	0.38	0.063	0.112	0.197	0.551
		MBS		0.31	0.042	0.089	0.139	0.191
		MTFA		0.36	0.071	0.151	0.235	0.321
X	BI-45°	MISDR	Long	0.42	0.169	0.418	1.028	5.244
			Short	0.48	0.078	0.162	0.335	1.248
		MBS		0.34	0.109	0.375	0.772	1.288
		MTFA		0.34	0.075	0.163	0.255	0.351

where μ is the median intensity measure and Δr is the total standard deviation.



(i) Slight



(ii) Moderate

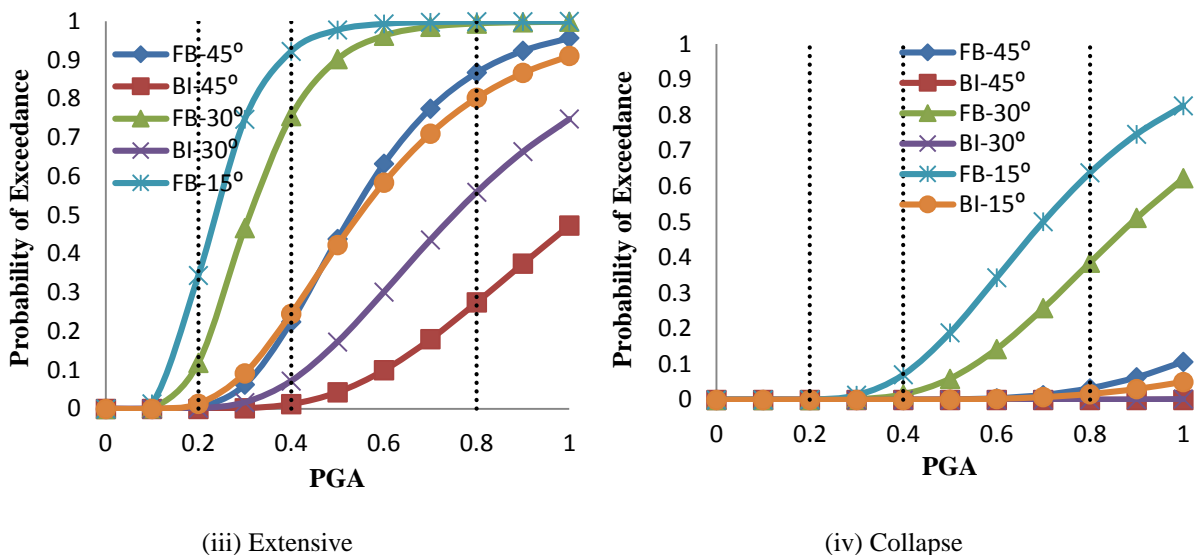
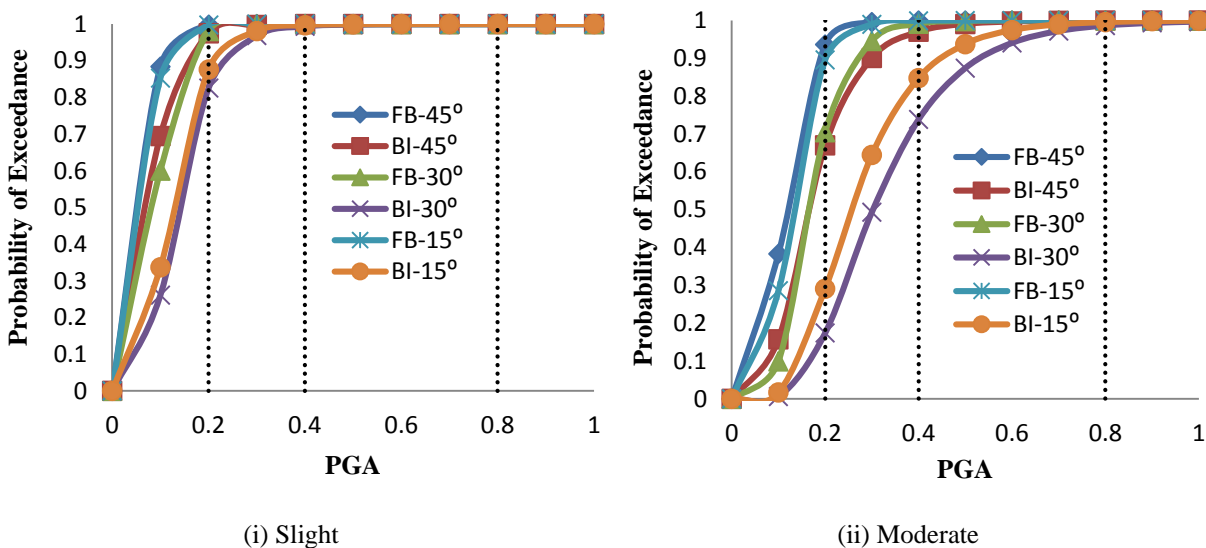


Fig. 5 Variation of fragility curves of Maximum inter-storey drift ratio of long column side along X-direction : (i) Slight (ii) Moderate (iii) Extensive and (iv) Collapse.

From Fig.5 along long column side the average percentage reduction in P_f of MISDR for BI-15° is 7.85%, 22.78%, 52.54% and 88.44%; for BI-30° is

8.53%, 29.36%, 69.39% and 79.93% and for BI-45° is 2.42%, 33.18%, 71.92% and 70% corresponding to slight, moderate, extensive and collapse damage states when compared to their FB counterparts.



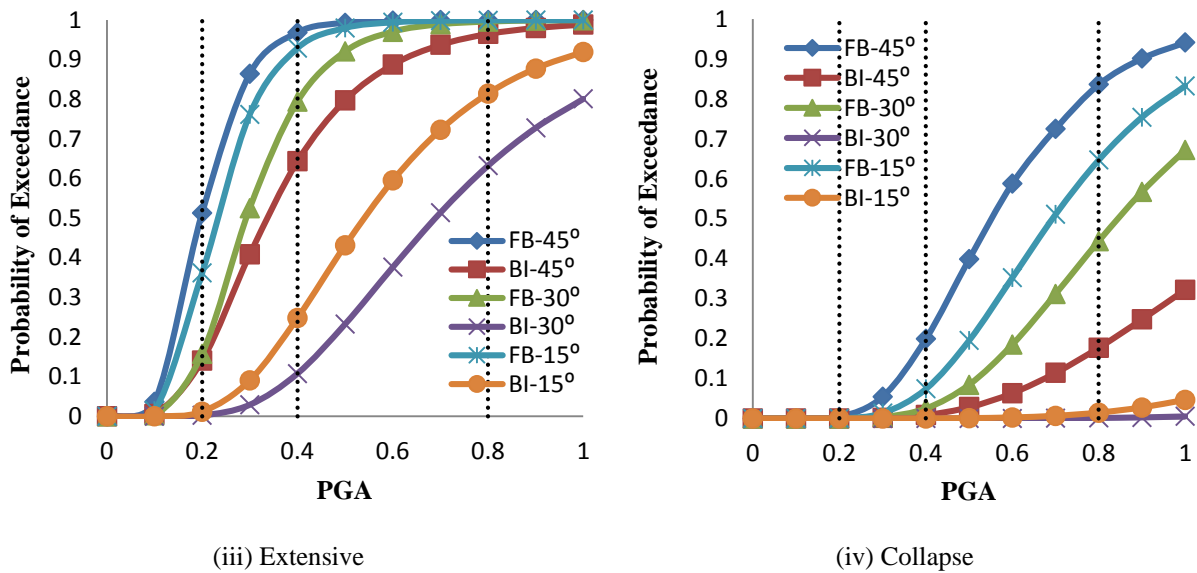
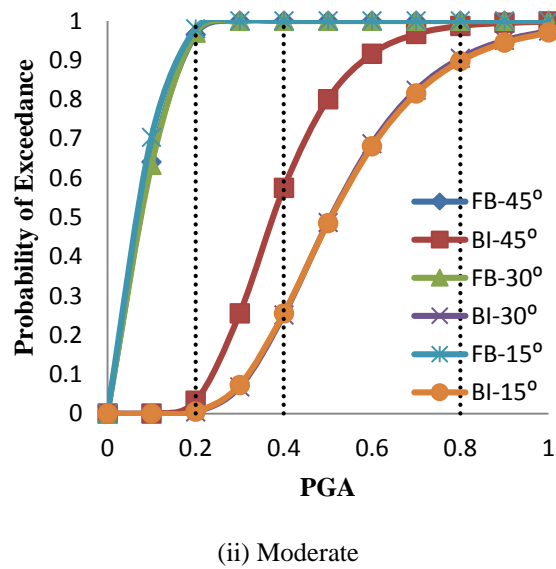
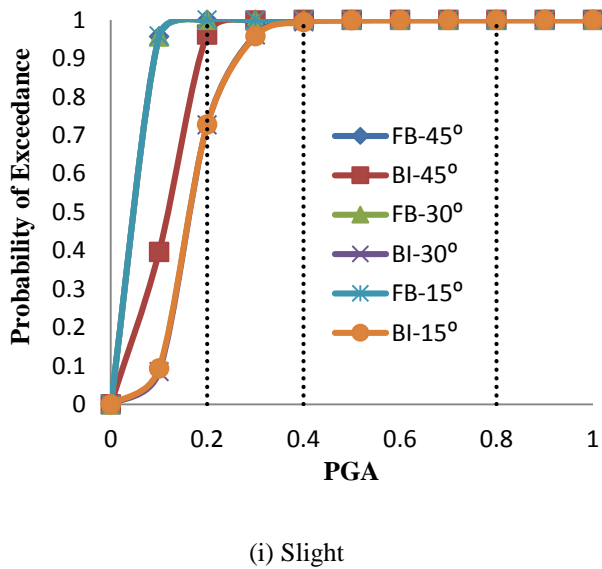
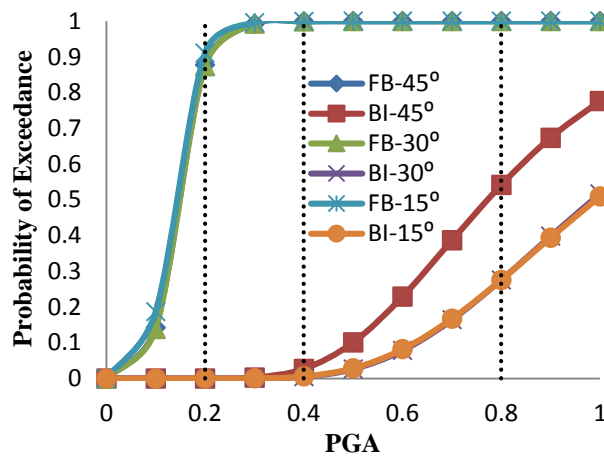


Fig. 6 Variation of fragility curves of Maximum inter-storey drift ratio of short column side along X-direction(i) Slight (ii) Moderate (iii) Extensive and (iv) Collapse.

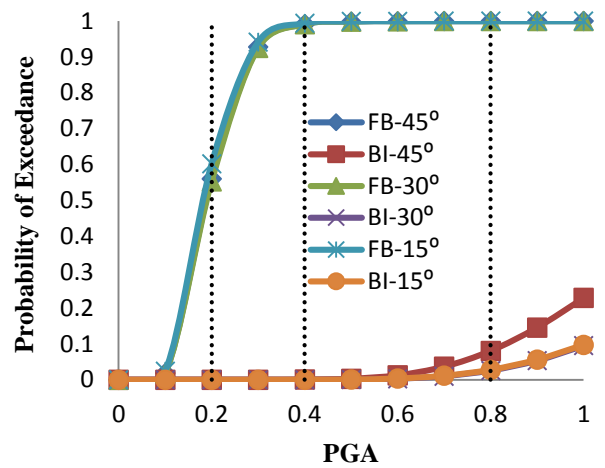
It has been observed that from Fig. 6, along short column side the average percentage reduction in P_f of MISDR for BI-15° is 7.49%, 22.24%, 52% and 88.62%; for BI-30° is 7.62%, 26.62%, 64.66% and

89.82% and for BI-45° is 2.41%, 10.13%, 28.62% and 77.36% corresponding to slight, moderate, extensive and collapse damage states when compared to their FB counterparts.





(iii) Extensive

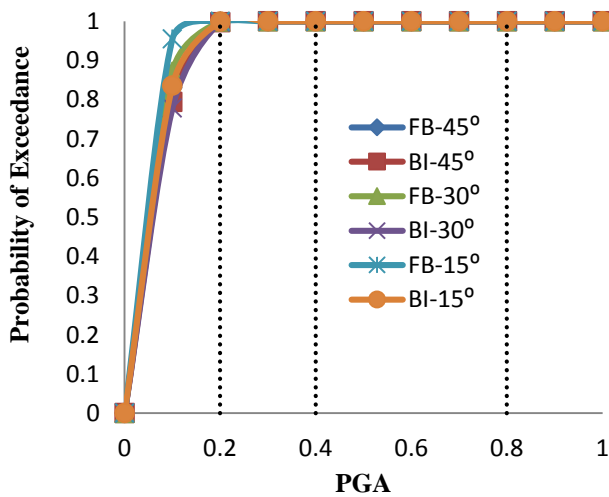


(iv) Collapse

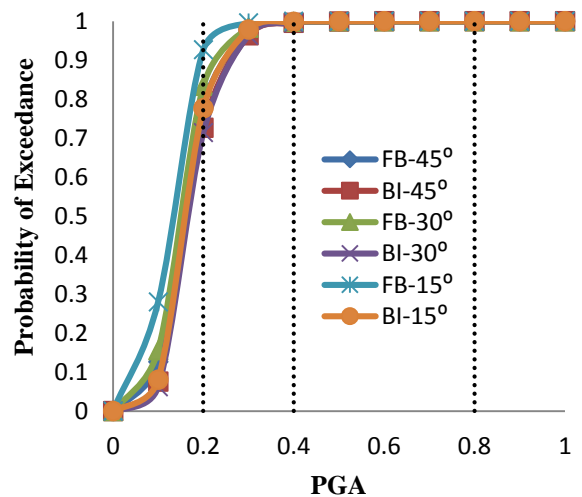
Fig. 7 Variation of fragility curves of Maximum base shear along X-direction (i) Slight (ii) Moderate (iii) Extensive and (iv) Collapse.

From Fig.7 the average percentage reduction in P_f of MBS for BI-15° is 12.25%, 48.75%, 85.36% and 98.04%; for BI-30° is 12.28%, 48.51%, 85.35% and 98.12% and for BI-45° is 6.25%, 34.74%, 72.64% and

94.94% corresponding to slight, moderate, extensive and collapse damage states when compared to their FB counterparts.



(i) Slight



(ii) Moderate

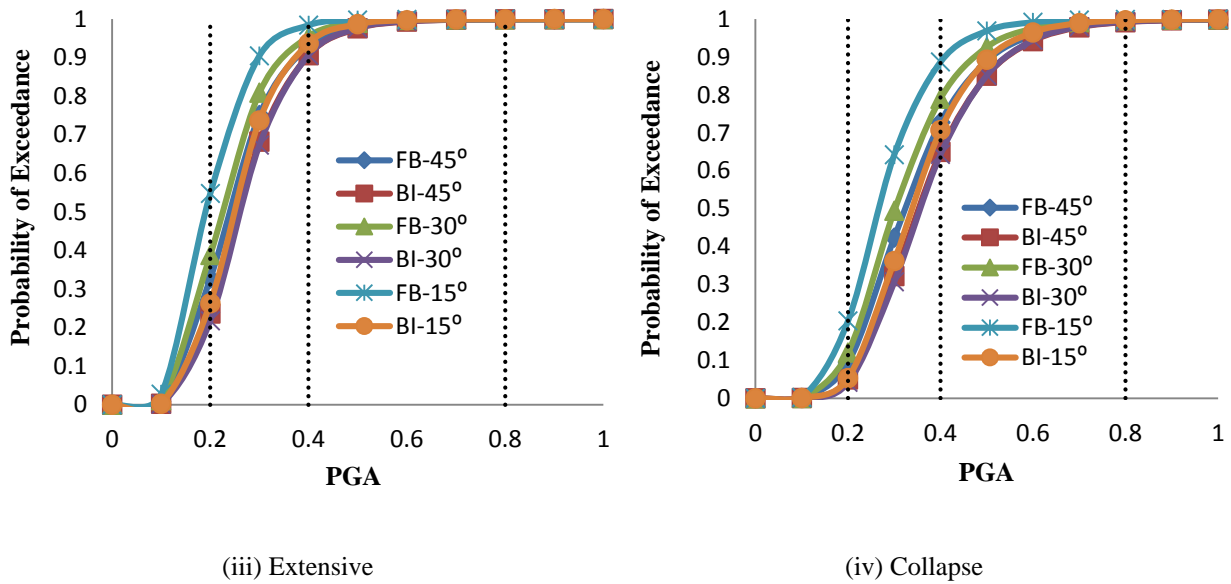
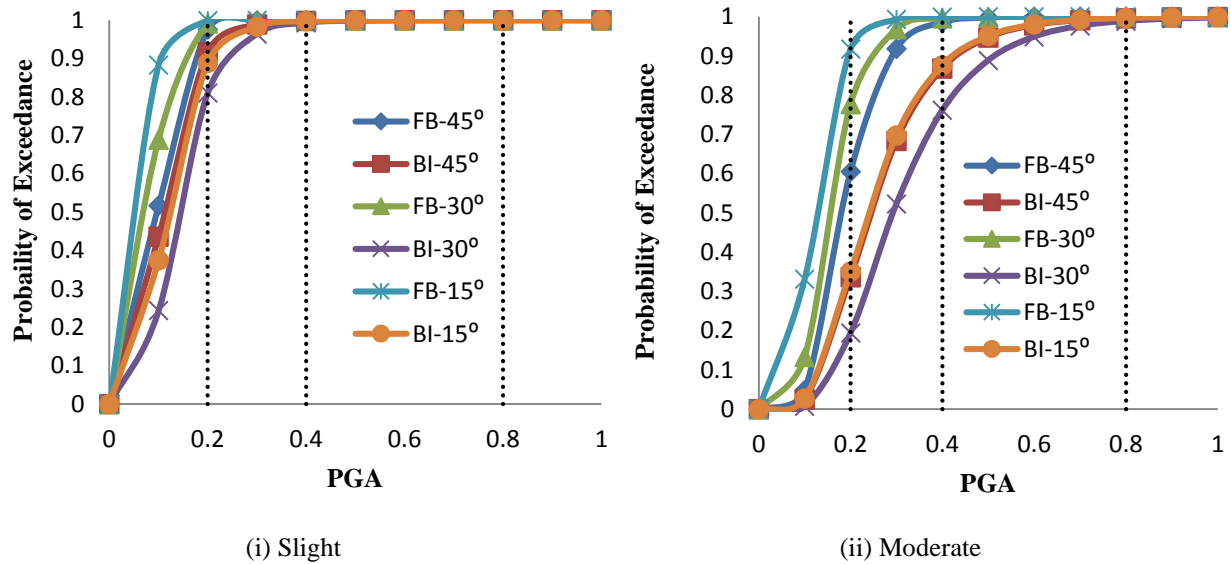
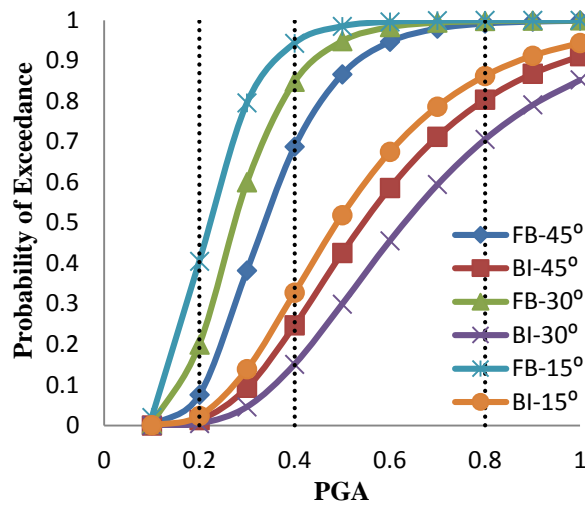


Fig. 8 Variation of fragility curves of Maximum top floor acceleration along X-direction (i) Slight (ii) Moderate (iii) Extensive and (iv) Collapse.

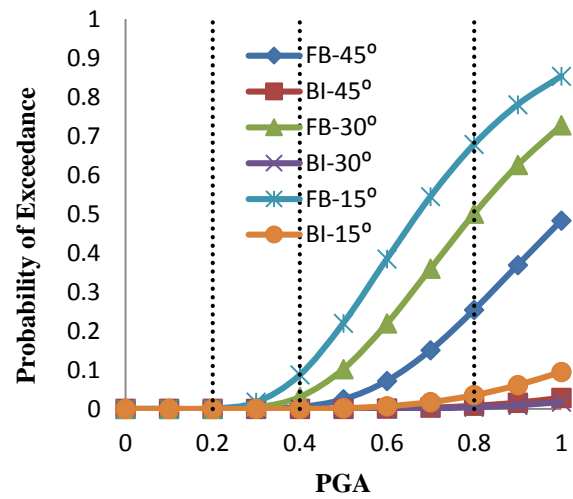
From Fig. 8 the average percentage reduction in P_f of MTFA for BI-15° is 1.26%, 8.95%, 16.70% and 24.52%; for BI-30° is 1.08%, 7.65%, 15.04% and

22.26% and for BI-45° is 0.44%, 4.83%, 10.7% and 17.24% corresponding to slight, moderate, extensive and collapse damage states when compared to their FB counterparts.





(iii) Extensive

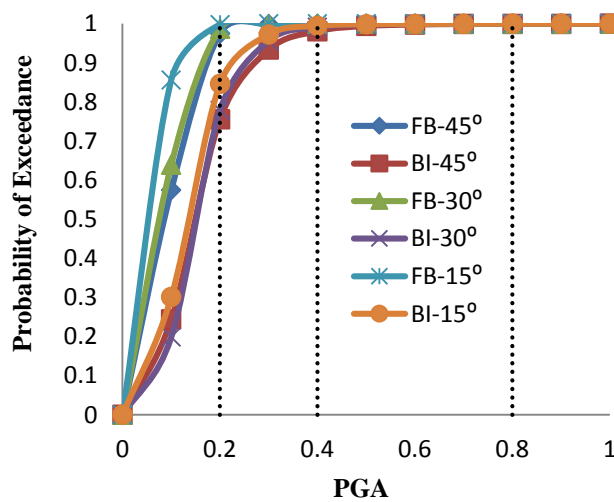


(iv) Collapse

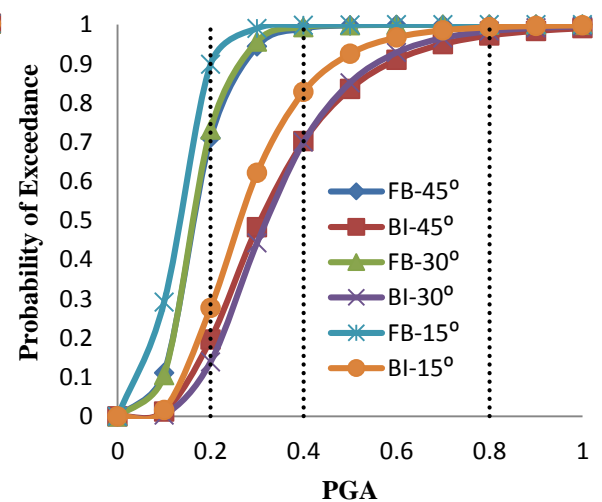
Fig. 9 Variation of fragility curves of Maximum inter-storey drift ratio of long column side along Y-direction(i) Slight (ii) Moderate (iii) Extensive and (iv) Collapse.

From Fig. 9 along long column side the average percentage reduction in P_f of MISDR for BI-15° is 7.06%, 20.4%, 47% and 86.92%; for BI-30° is 8.73%,

25.96%, 59.95% and 89.42% and for BI-45° is 2.29%, 13.95%, 45.45% and 78.13% corresponding to slight, moderate, extensive and collapse damage states when compared to their FB counterparts.



(i) Slight



(ii) Moderate

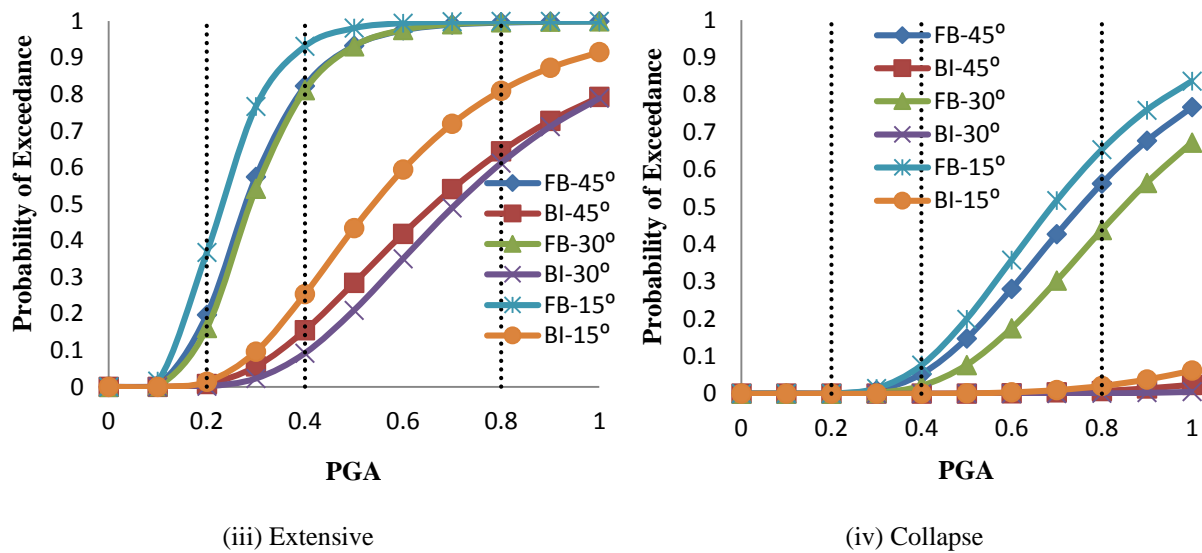


Fig. 10 Variation of fragility curves of Maximum inter-storey drift ratio of short column side along Y-direction (i) Slight (ii) Moderate (iii) Extensive and (iv) Collapse.

From Fig. 10 along short column side the average percentage reduction in P_f of MISDR for BI-15° is 8.34%, 23.09%, 52% and 88.07%; for BI-30° is 9.54%, 28.88%, 66.41% and 79.82% and for BI-45° is 8.92%, 27.45%, 62.02% and 89.17% corresponding to slight, moderate, extensive and collapse damage states when compared to their FB counterparts.

Whenever there is a difference in the height of columns due to the slope of the ground, there is a tendency that the shorter side is more vulnerable than the longer one. In order to verify the statement, the variation of MISDR of the shorter side and the longer side of the FB buildings inclined at 15°, 30° and 45° is being plotted with the help of fragility curves for extensive and collapse damage states.

1.5 Conclusions

Probabilistic estimation of structural vulnerability is essential owing to the uncertain nature of earthquakes as well as structural capacity. Fragility analysis helps to correlate demand and capacity in order to establish probabilistic characterization of the demand measures against specified limits. A comparative study of buildings with fixed base and flexible base situated on sloping ground has been presented under the impacts of near earthquakes by means of fragility curves. The following conclusions have been drawn based on the present study:

- The median value or the threshold value of all the three damage parameters namely MISDR along long and short column direction, MBS and MTFA of BI building is more than FB for all the four damage states in both X and Y-direction. Therefore, it can be inferred that buildings with flexible base

can withstand earthquakes with greater intensity in contrast to FB.

- Along long column side the average percentage reduction in P_f of MISDR for BI-15° is 88.44%; for BI-30° is 79.93% and for BI-45° is 70% corresponding to collapse damage state in X-direction and in Y-direction for BI-15° it is 86.92%; for BI-30° is 89.42% and for BI-45° is 78.13% when compared to their FB counterparts.
- Along short column side the average percentage reduction in P_f of MISDR for BI-15° is 88.62%; for BI-30° 89.82% and for BI-45° is 77.36% corresponding to extensive and collapse damage state in X-direction while in Y-direction for BI-15° it 88.07%; for BI-30° is 79.82% and for BI-45° 89.17% for the similar damage state.
- The average percentage reduction in P_f of MBS for BI-15° is 98.04%; for BI-30° is 98.12% and for BI-45° 94.94% in X-direction corresponding to collapse state of damage.
- The average percentage reduction in P_f of MTFA for BI-15° is 24.52%; for BI-30° is 22.26% and for BI-45° is 17.24% in X-direction corresponding to the similar damage state.
- For buildings on 15°, 30° and 45° slopes, the shorter side of the columns showed more vulnerability than the longer side in terms of MISDR and the most critical slope was 45°.

References

- Baker, J.W., & Cornell, A. (2006), Vector –Valued ground motion intensity measures for probabilistic seismic demand analysis, (Report No. 150), PEER Report - 2006 Pacific Earthquake Engineering Research Center, College of Engineering, Univ. of California.
- Birajdar, B.G., & Nalawade, S.S. (2004), Seismic analysis of buildings resting on sloping ground, *In: 13th world Conference on Earthquake Engineering*, Vancouver, B. C., Canada.
- BIS (Bureau of Indian Standards) (2016), Criteria for Earthquake Resistant Design of Structures, IS 1893(Part 1):2016. Manak Bhawan, India: BIS.
- Bhandari, M., Bharti, S.D., Shrimali, M.K., & Datta, T.K. (2019). Seismic Fragility Analysis of Base-Isolated Building Frames Excited by Near- and Far-Field Earthquakes. *J. Perform. Constr. Facil.*, 2019, 33(3): 04019029.
- Chopra, A.K. (1981), *Dynamics of Structures: Theory and Applications to Earthquake Engineering*, University of California at Berkeley.
- Center for Engineering Strong Motion Data. Retrieved from (<http://www.strongmotioncenter.org>), USGS.
- Darji, R.V, and Purohit, S.P. (2006), Design of base isolator for RCC building and performance evaluation, *Conference Paper*-January 2006.
- Duggal, S.K. (2013), *Earthquake Resistant Design of Structures*, Oxford University Press.
- Ellingwood, B.R., & Kinali, K. (2009), Quantifying and communicating uncertainty in seismic risk assessment, *Structural Safety*, Vol. 31, No.2, Pages 179-187.
- FEMA. (2000), Prestandard and commentary for the seismic rehabilitation of buildings, FEMA 356. Washington, DC: SAC Joint Venture, FEMA.
- FEMA P-58. (2012), Seismic Performance assessment of buildings Vol.-1 methodology, Redwood City, California.
- Ghosh, S, Ghosh, S & Chakraborty, S. (2017), Seismic fragility analysis in the probabilistic performance-based earthquake engineering framework: an overview, *International Journal of Advanced Engineering Science and Applied Mathematics*, <https://doi.org/10.1007/s12572-017-0200-y>.
- Gomase, O.P, & Bakre, S.V. (2011,) Performance of non-linear elastomeric base-isolated building structure, *International Journal of Civil and Structural Engineering*, 2(1):280-291.
- Heydari, M, & Mousavi, M. (2015), The Comparison of seismic effects of near-field and far-field earthquakes on relative displacement of seven-storey concrete building with shear wall, *Current World Environment*, 10(1): 40-46.
- Hwang, H.H.M, & Low, Y.K. (1989), Seismic reliability analysis of plane frame structures, *Probabilistic Engineering Mechanics*, 4(2):74-84.
- Jangid, R.S, & Kelly, J.M. (2001), Base isolation for near-fault motions, *Earthquake Engineering and Structural Dynamics*, 30: 691-707.
- Keerthan, S. Kumar, S, Balamonica, K. & Jagannathan, D.S. (2014), Seismic response control using base isolation strategy, *International Journal of Emerging Technology and Advanced Engineering*, 4(4):77-81.
- Naeim, F. & Kelly, J.M. (1999), *Design of Seismic Isolated Structures: From Theory to Practice*, New York: Wiley.
- Rani, A. & Singh, V. (2018), A parametric study on the fragility analysis of fixed base and flexible base structure under earthquake forces, *International Research Journal of Engineering and Technology*, 5(5): 4174-4184.
- Reed, J.W. & Kennedy, R.P. (1994), Methodology for developing seismic fragilities, (Report No. TR-103959), California: Electric Power Research Institute.
- Robinson, W.H. (1982), Lead-rubber hysteric bearings suitable for protecting structures during Earthquakes, *Earthquake Engineering and Structural Dynamics*, 10(4): 593-604.
- Salic, R.B., Garevski, M.A., & Milutinovic, Z.V. (2008), Response of lead-rubber bearing isolated structure, *In: 14th world Conference on Earthquake Engineering*, (2008), Beijing, China.
- Shah, H.J. (2014), Seismic time history analysis of buildings on sloping ground considering near/far field earthquakes, *International Journal of Engineering Research and Technology*, 3(3):982-986.
- Shinozuka, M. Feng, M., Lee, J. & Toshihiko, Naganuma T. (2000), Statistical analysis of fragility curves, *Journal of Engineering Mechanics*, 126(12): 1224-1231.
- Shome, N. & Allin, Cornell C. (1999), Probabilistic seismic demand analysis of nonlinear structures, (Technical Report, RMS-35), RMS Program, Stanford University, CA.
- Sumana, C.V., Raghu, M.E. & Harugoppa, R. (2016), Comparative study on fixed base and base isolated buildings on sloping ground, *International Journal of Innovative Research in Science, Engineering and Technology*, 5(8):14955-14971.
- Uniform Building Code 1997- Vol. 2, *by International Conference of Building Officials, Whittier, California.*
- Vamvatsikos, D. & Cornell, C.A. (2002), Incremental dynamic analysis, *Earthquake Engineering and Structural Dynamics*, 31(3): 491-514.
- Funding Acknowledgement: This research received no specific grant from any funding agency in the public, commercial, or not-for-profit sectors.
- Conflict of interest statement: The authors declare no conflict of interest in preparing this article.